Effect of iron addition on the durability of Pd–Pt-loaded sulfated zirconia for the selective reduction of nitrogen oxides by methane

Hirofumi Ohtsuka *

Research and Development Department, Osaka Gas Co. Ltd, 6-19-9 Torishima, Konohana-ku, Osaka 554-0051, Japan

Received 14 November 2002; accepted 10 February 2003

The effects of adding iron to Pd–Pt/sulfated zirconia (SZ) on the selective NO_x reduction by methane were examined based on durability tests under conditions simulating natural gas combustion exhaust. While Pd–Pt/SZ was severely deactivated at 500 °C, Pd–Pt/Fe-SZ maintained a NO_x conversion higher than 70% for over 2400 h under the same conditions. Methane conversion on Pd–Pt/Fe-SZ was significantly lower than that on Pd–Pt/SZ. XRD analysis of fresh and used catalysts showed that a part of the SZ had transformed to monoclinic ZrO_2 and that adding Fe suppressed the transformation. These results suggested that the improvement in NO_x conversion by adding Fe was due to the suppression of methane combustion and the stabilization of SZ against transformation to ZrO_2.

KEY WORDS: NO_x reduction; palladium; platinum; sulfated zirconia; methane.

1. Introduction

In the last decade intense research has been devoted to the selective catalytic reduction of nitrogen oxides (NO_x) by hydrocarbons in the presence of excess oxygen. Two decades have passed since the selective catalytic reduction of NO_x by ammonia (ammonia-SCR) was commercially applied to NO_x reduction from oxygen-rich exhaust. However, because this method requires a supply of reductants, such as ammonia or urea solutions, and is expensive to avoid ammonia slip, its use is still mostly limited to large-scale applications, such as power plants and municipal waste incinerators. The selective catalytic reduction of NO_x by hydrocarbons is considered a potential NO_x reduction process for small-scale stationary emission sources and mobile emission sources. Methane is the main component of natural gas, and its supply through pipelines is established in many countries. Therefore, using methane as a reductant has a great advantage in terms of reductant supply.

Ion exchanged zeolite catalysts such as Co-MFI [1], Ni-MFI [2], Ga-MFI [3,4], In-MFI [3], Pd-MFI [5,6], and Pd-MOR [7] have been reported as catalysts for the selective catalytic reduction of NO_x by methane. However, most of these catalysts are severely affected by water vapor, which is inevitably contained in the exhaust produced by the combustion of fossil fuels, and show only marginal activity at temperatures below 500 °C [5,8]. Pd-loaded zeolite shows an activity of a practical level even in the presence of 10 vol% water vapor at 400 °C [7], but undergoes almost complete deactivation in a few days [9]. To improve the durability of Pd-loaded zeolite, silica deposition on the external surface of zeolite crystals [10] and the incorporation of a second metal [11,12] have been proposed.

Various acidic oxides other than zeolite have also been reported to be active for the reaction [13,14]. Resasco *et al.* reported that sulfated zirconia and tungstated zirconia loaded with Pd are active for the reduction of NO_x by methane [15,16].

In actual exhaust, sulfur oxides (SO_x) which originate from organic sulfur compounds in the fuel are present mainly as sulfur dioxide (SO_2). This is known as a strong poison in the combustion of hydrocarbons on Pd-based catalysts [17]. The author has reported that sulfated zirconia (SZ) loaded with Pd and Pt maintained stable activity in the presence of water vapor and SO_2, while Pd-MOR rapidly deactivated under the same conditions [18]. While SO_2 accelerated the deactivation of Pd-MOR, it stabilized the activity of Pd–Pt/SZ. Since surface sulfate plays a key role in the reaction and it can desorb as SO_x at high temperatures, it was suggested that the presence of SO_2 stabilized the surface sulfate, which led to the stabilization of activity.

Further investigation revealed that adding iron to SZ remarkably improved the stability of Pd–Pt/SZ even at low SO_2 concentrations. The effects of iron on the acidity and *n*-butane isomerization activity of SZ [19,20] and the state of iron in Fe-SZ [21,22] have already been reported, but little is known about the effects on NO_x reduction. This paper reports the effects of iron on the selective NO_x reduction by methane on Pd–Pt/SZ based on durability test results under conditions simulating natural gas combustion exhaust.

* To whom correspondence should be addressed.
E-mail: ohtsuka@osakagas.co.jp

1011-372X/03/0400-0179/0

2. Experimental

2.1. Catalyst preparation

SZ was prepared by immersing 180 g of zirconium hydroxide (79% as ZrO_2, Mitsuwa Chemical, Osaka) in a solution in which 27 g of ammonium sulfate (Hayashi Pure Chemicals, Osaka) were dissolved. The mixture was dried and calcined in air at 550 °C. X-ray diffraction (XRD) analysis revealed that the SZ mostly consisted of the tetragonal phase. Iron-loaded SZ (Fe-SZ) was prepared in a similar manner. For example, 0.93% Fe-SZ was prepared using a solution in which 27 g of ammonium sulfate, 7.5 g of iron sulfate ($FeSO_4 \cdot 7H_2O$, Kanto Chemical, Tokyo), and 1.4 g of sulfuric acid (95%, Kanto Chemical) were dissolved. Sulfuric acid was added to avoid the precipitation of iron(III) hydroxide when the iron(II) cation was oxidized by atmospheric oxygen. Palladium and platinum were loaded by impregnation using aqueous solutions prepared from $Pd(NO_3)_2$ and $Pt(NH_3)_4(NO_3)_2$ (N. E. Chemcat, Tokyo). The impregnated solid was dried and calcined in air at 500 °C. Throughout this preparation, Pd loading was 0.25 wt% and Pt loading was 0.1 wt%. The loadings are in nominal wt% calculated from the amount of metal in the solution and the amount of support (SZ or Fe-SZ).

As reference materials for Raman measurement, the following commercial samples were used: ZrO_2 ($42\,m^2\,g^{-1}$, N. E. Chemcat), α-Fe_2O_3 (99.97%, Kishida Chemicals, Osaka), PdO (99.9%, Kanto Chemical). Because the SZ prepared by the method described above was too fluorescent to obtain a usable spectrum, another SZ was prepared by a slightly different method: zirconium hydroxide was contacted with a 0.75 M H_2SO_4 solution, and the solid was separated by filtration and calcined at 600 °C. It was confirmed by XRD that the SZ almost solely consisted of the tetragonal phase. This SZ was only used as a reference for Raman measurement.

2.2. Durability tests

Durability tests of the catalysts were carried out using a fixed-bed flow reactor. Details of the catalytic activity measurements are similar to those described elsewhere [18]. The catalyst was formed into pellets, crushed, and sieved into 1–2 mm grains. The sieved catalyst (4 ml) was placed in a quartz reactor (14 mm i.d.). A reaction gas was fed at a rate of $1\,l\,min^{-1}$, which corresponded to a GHSV of $15\,000\,h^{-1}$. The gas compositions were: NO 150 ppm, CH_4 2000 ppm, O_2 10%, H_2O 9%, CO_2 6%, SO_2 0.3 ppm, and the balance N_2. The concentrations of O_2, H_2O, CO_2, and SO_2 were intended to simulate the exhaust of natural gas combustion at an excess air ratio (λ) of 2, which means that the air/fuel ratio was twice that of stoichiometric combustion. The NO and NO_2 concentrations were measured by a chemiluminescence NO_x analyzer equipped with an NO_2 converter (Yanaco Analytical Systems, Kyoto). The CH_4 concentration was measured by a gas chromatograph (Yanaco Analytical Systems). NO_x conversion was defined by $1 - (\text{outlet } NO_x)/(\text{inlet } NO_x)$, and methane conversion was defined by $1 - (\text{outlet } CH_4)/(\text{inlet } CH_4)$.

2.3. Catalyst characterization

BET surface area measurements were carried out using an automatic BET surface area analyzer (AMS-8000, Ohkura Riken, Tokyo). The amount of N_2 adsorption was measured at 77 K, $P/P_0 = 0.3$, and the surface area was calculated according to the one point method.

XRD was measured using a Rigaku RAD-2B diffractometer using Ni-filtered CuKα radiation. Raman spectra were measured using a Spex 1877 triple polychromator equipped with a liquid N_2-cooled CCD detector (Princeton Instruments, CCD-1752PBUV) at a spectral resolution of *ca.* $3\,cm^{-1}$. A 532 nm radiation from a diode-pumped Nd:YAG laser (Coherent, DPSS 532-50) was used for excitation. A filter spectrometer (Spectrolab, Laserspec III) was used. The incident laser power was kept between 5 and 10 mW at the sample and the back-scattered Raman signal was recorded. All measurements were carried out under ambient conditions without any pretreatment of the samples.

The sulfur content of the sample was determined by ICP. The sample was treated with a 1:1 mixture of concentrated HCl and deionized water, and the sulfur in the solution was analyzed by ICP. The iron content of the sample was measured by X-ray fluorescence using a Rigaku RIX-3100 analyzer.

The fraction of the dispersed Pd was determined according to the method of Ogura *et al.* [23]. Briefly, about 0.5 g of the powder sample was added to a 0.2 M NaCl solution (30 ml) and kept at 80 °C for 1.5 h under constant stirring. After filtration, the Pd content in the filtrate was determined by ICP. The fraction of the dispersed Pd was calculated assuming that the eluted Pd corresponded to the dispersed Pd.

3. Results

3.1. Effects of iron addition

Figure 1(a) shows the change of NO_x and methane conversions with time on stream over Pd–Pt/SZ at 450 °C. NO_x conversion was 58% initially, but decreased to 43% after 90 h, and further decreased to 29% after 500 h. Methane conversion was 60% initially, but decreased to 37% after 90 h, and further decreased to 30% after 500 h. On 0.38% Pd–0.12% Pt/SZ, initial NO_x conversion of *ca.* 60% decreased to 38% after 80 h in the absence of SO_2, while it was stable at 50–55% for

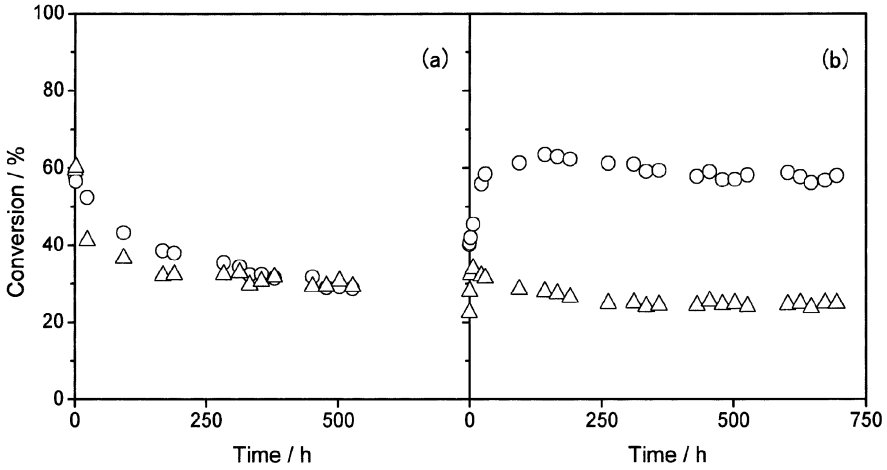

Figure 1. Changes in NO_x and methane conversion with time on stream over (a) 0.25% Pd–0.1% Pt/sulfated zirconia and (b) 0.25% Pd–0.1% Pt/0.93% Fe-sulfated zirconia at 450 °C. Reaction conditions: NO 150 ppm, CH_4 2000 ppm, O_2 10%, CO_2 6%, H_2O 9%, SO_2 0.3 ppm, GHSV 15 000 h^{-1}. ○: NO_x conversion; △: methane conversion.

over 100 h in the presence of 3 ppm SO_2 [18]. The deactivation under a SO_2 concentration of 0.3 ppm is similar to that observed in the absence of SO_2. Since the SO_2 concentration in natural gas combustion exhaust usually does not exceed 1 ppm, the results suggest that Pd–Pt/SZ is not sufficiently durable under actual conditions.

Figure 1(b) shows the change of NO_x and methane conversions with time on stream over Pd–Pt/0.93% Fe-SZ at 450 °C. NO_x conversion was 40% initially, but increased to 60% after 100 h, and remained at around 60% up to 700 h. Methane conversion showed a similar change over time. The stability of NO_x conversion was greatly improved compared with the results of Pd–Pt/SZ.

Figure 2(a) shows NO_x and methane conversion over Pd–Pt/SZ at 500 °C. NO_x conversion reached a maximum of 50% after 4 h and decreased to 19% after 340 h. Methane conversion was 92% initially, decreased to 85% after 20 h, and became stable at *ca.* 90% after 100 h. While the NO_x conversion showed a large decrease, the change in methane conversion was small, which means that the selectivity for NO_x reduction decreased with time on stream.

The result on Pd–Pt/0.93% Fe-SZ is shown in figure 2(b). A remarkable NO_x conversion of higher than 70% was maintained for more than 2400 h. The NO_x conversion (70%) exceeds the maximum NO_x conversion obtained on Pd–Pt/SZ (*ca.* 60% at 450 °C [24]). Methane conversion showed a gradual decrease with time but became almost constant at 55% after 1600 h. An increase in NO_x conversion at the initial stage was also observed at 500 °C.

Under identical conditions, the activities of SZ and 0.93% Fe-SZ for NO_x reduction were low. The NO_x and methane conversions on SZ at 500 °C were 8 and 1%, respectively. The activity of Fe-SZ gradually increased and became almost constant after 20 h on stream. NO_x and methane conversions over Fe-SZ after 100 h on stream were 13 and 4%, respectively.

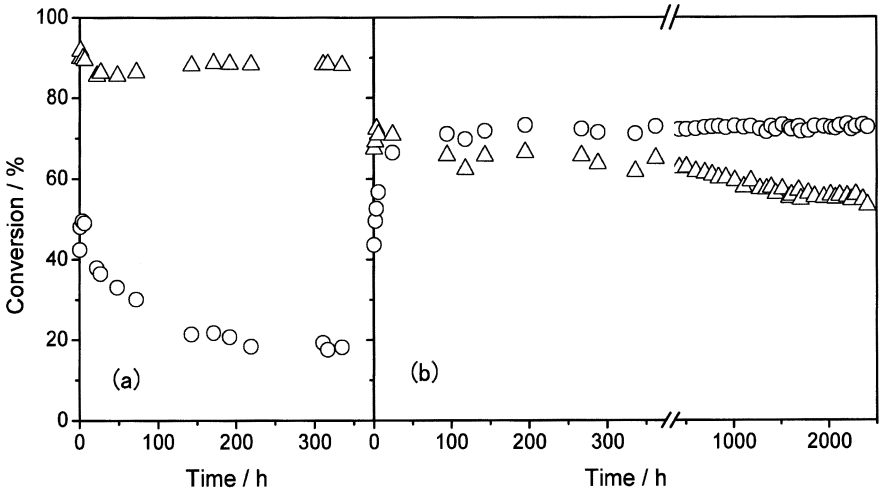

Figure 2. Changes in NO_x and methane conversion with time on stream over (a) 0.25% Pd–0.1% Pt/sulfated zirconia and (b) 0.25% Pd–0.1% Pt/0.93% Fe-sulfated zirconia at 500 °C. Reaction conditions and symbols as in figure 1.

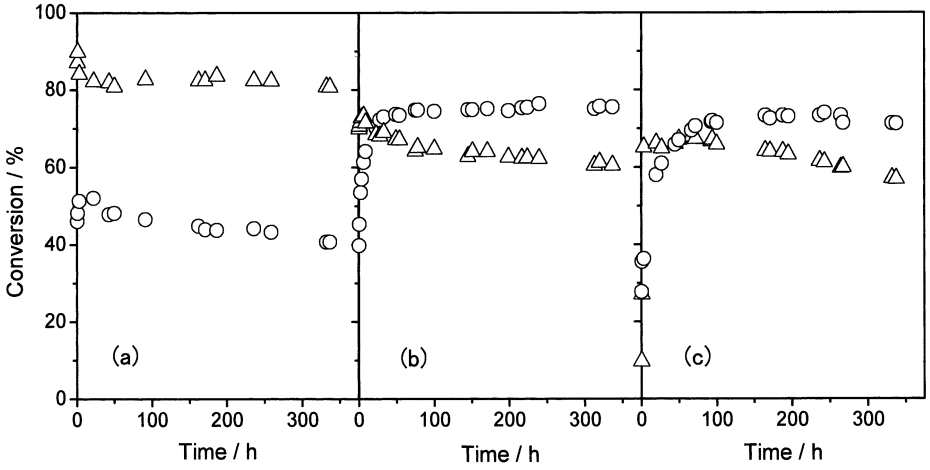

Figure 3. Changes in NO_x and methane conversion with time on stream over 0.25% Pd–0.1% Pt/Fe-doped sulfated zirconia at 500 °C. Fe content: (a) 0.46 wt%, (b) 1.8 wt%, (c) 3.9 wt%. Reaction conditions and symbols as in figure 1.

3.2. *Effects of iron concentration*

Figure 3 shows the changes of NO_x and methane conversions with time on stream over Pd–Pt/0.46% Fe-SZ, Pd–Pt/1.8% Fe-SZ, and Pd–Pt/3.9% Fe-SZ at 500 °C. Over Pd–Pt/0.46% Fe-SZ, a maximum NO_x conversion of 52% was observed after 20 h on stream. The initial NO_x conversion (0.5 h on stream) was 46%, and the difference was 6%. The NO_x conversion after 340 h on stream was 41%, and a deactivation in NO_x reduction was clearly observed, although the deactivation was much smaller than that observed over Pd–Pt/SZ. Methane conversion over Pd–Pt/0.46% Fe-SZ slightly decreased with time in the initial 20 h, but it became almost constant after that. It should be noted that both the NO_x and methane conversions over Pd–Pt/0.46% Fe-SZ were intermediate between those of Pd–Pt/SZ and Pd–Pt/0.93% Fe-SZ in terms of both the value and the change over time.

The NO_x conversion over Pd–Pt/1.8% Fe-SZ became stable at *ca.* 75% after 50 h on stream. The initial NO_x conversion (0.5 h on stream) was 40%, and the difference was 35%. About 100 h was required for the stabilization of NO_x conversion over Pd–Pt/3.9% Fe-SZ. The initial NO_x conversion was 27%, and the maximum was 74%. The difference was 47%. Methane conversion was 10% initially, but it increased sharply and became 65% after 3.5 h on stream.

The results over catalysts with various Fe concentrations are summarized as follows. Methane conversion decreased as Fe concentration increased, but up to 1.8 wt%. NO_x conversion became maximum at a Fe concentration of 1–2 wt%. The addition of Fe caused an induction period in NO_x conversion. The time required for the full activation and the difference in NO_x conversion before and after activation increased as Fe concentration increased.

3.3. *Characterization results of fresh and used catalysts*

Table 1 shows the results of chemical analysis of the fresh and used catalysts as well as the supports. While the Fe concentration in the support was almost in agreement with the nominal content calculated by the equation $Fe/(Fe_2O_3 + SO_3 + ZrO_2)$, based on the amount of used $FeSO_4$, H_2SO_4, $(NH_4)_2SO_4$, and zirconium hydroxide, the S concentration by analysis was significantly lower than nominal values calculated by the

Table 1
Chemical composition of the supports and the catalysts

	Support		Fresh catalyst, S (wt%)	Used catalyst, S (wt%)
	Fe (wt%)	S (wt%)		
Pd–Pt/SZ		2.5 (4.0 [a])	2.4	0.28 [b]
Pd–Pt/0.46% Fe-SZ	0.46 (0.43 [a])	2.6 (4.3 [a])	2.5	0.42 [b]
Pd–Pt/0.93% Fe-SZ	0.93 (0.85 [a])	3.6 (4.6 [a])	3.5	0.27 [b]
Pd–Pt/1.8% Fe-SZ	1.8 (1.7 [a])	4.2 (5.2 [a])	3.8	0.51 [b]
Pd–Pt/3.9% Fe-SZ	3.9 (3.7 [a])	6.3 (6.6 [a])	5.8	0.90 [b]

[a] Nominal content.
[b] After durability test at 500 °C.

equation $S/(Fe_2O_3 + SO_3 + ZrO_2)$, especially at lower Fe concentrations. This is because a significant quantity of sulfate was lost during calcination. The ratio of (actual S content)/(nominal S content) on SZ was 0.63, but the values on 0.93% SZ and 3.9% Fe-SZ were 0.78 and 0.95. This suggests the stabilization of sulfate by Fe.

Fresh Pd–Pt/SZ contained 2.4 wt% S, which is close to the value of the parent SZ (2.5 wt%). This indicates that loaded sulfur is almost entirely retained during Pd–Pt impregnation and calcination at 500 °C. Pd–Pt/SZ after the 340 h test at 500 °C contained only 0.28% S, which means that a significant number of the acid sites were lost during the test.

The S content of used Pd–Pt/Fe-SZ samples also showed a large decrease. A comparison of the S content of Pd–Pt/SZ, Pd–Pt/0.46% Fe-SZ, Pd–Pt/1.8% Fe-SZ, and Pd–Pt/3.9% Fe-SZ, which were subjected to durability tests of 340 h, shows that the remaining S increased as Fe concentration increased. This result also suggests the stabilization of sulfate by Fe. It must be noted, however, that Pd–Pt/0.93% Fe-SZ after the 2400 h test at 500 °C contained only 0.27% S, which is almost the same as that of Pd–Pt/SZ.

Table 2 shows the BET surface area of the fresh and used catalysts as well as the supports. The addition of Fe did not cause a significant effect on the surface area of the supports, and Fe-doped SZ showed similar BET surface areas to SZ.

Figure 4(A) shows the XRD traces of the supports. The XRD of SZ consisted of the tetragonal phase as indicated by the strong peaks at $2\theta = 30°$, 35°, 50°, and 60°. Small amounts of the monoclinic phase were present as indicated by the peak at 28°. The XRD of 0.46% Fe-SZ was almost the same as that of SZ. At a Fe concentration of 0.93% or higher the amount of the monoclinic phase is negligible as shown by the 28° peak intensity. In addition, the peak heights became small, and a broad background appeared. At the Fe content in these samples (below 4 wt%), the change in the CuKα absorption coefficient is below 10%, which does not explain the large decrease in the peak intensities. Therefore, the decrease in the peak heights suggests the retardation of crystallization by Fe.

Figure 4(B) shows the XRD traces of the fresh catalysts. The intensities of the 28° peak increased compared with those of the corresponding supports. This indicates that a small part of the tetragonal phase turned into the monoclinic phase after Pd–Pt impregnation and calcination.

Table 2
BET surface area of the supports and the catalysts

	Support ($m^2\,g^{-1}$)	Fresh catalyst ($m^2\,g^{-1}$)	Used catalyst [a] ($m^2\,g^{-1}$)
Pd–Pt/SZ	124	101	72
Pd–Pt/0.46% Fe-SZ	118	104	71
Pd–Pt/0.93% Fe-SZ	133	108	67
Pd–Pt/1.8% Fe-SZ	122	105	87
Pd–Pt/3.9% Fe-SZ	110	93	86

[a] After durability test at 500 °C.

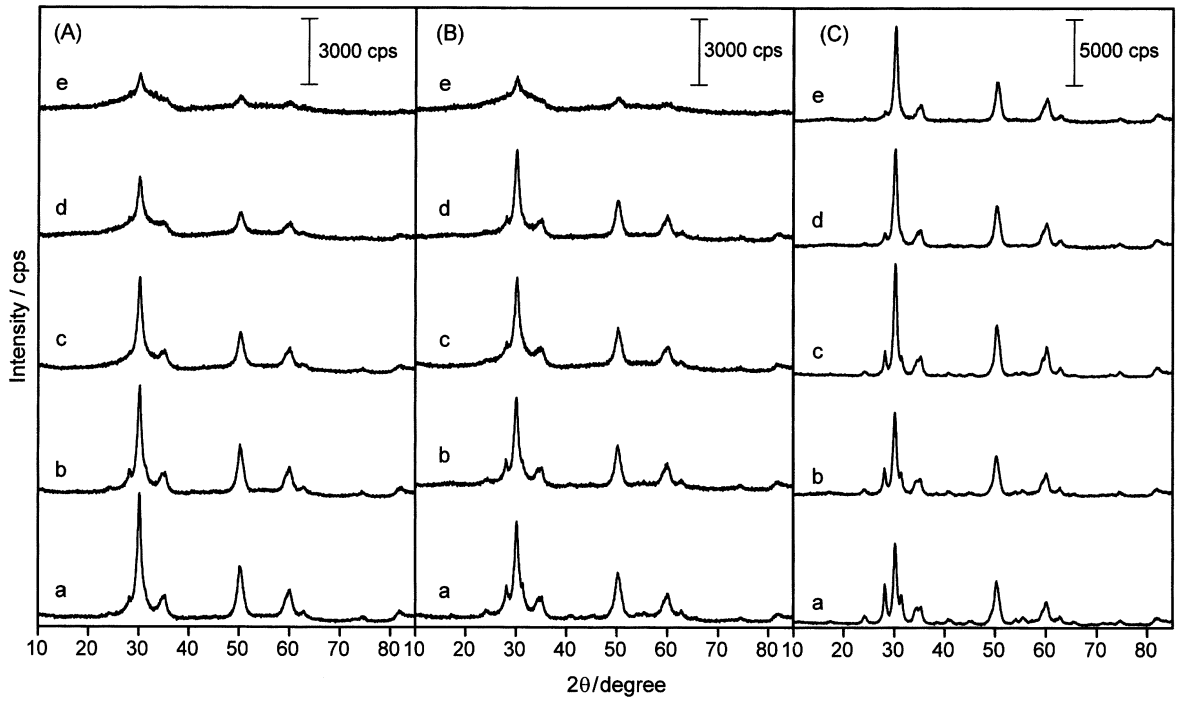

Figure 4. XRD patterns of (A) sulfated zirconia, (B) fresh Pd–Pt/sulfated zirconia, and (C) Pd–Pt/sulfated zirconia after reaction tests at 500 °C. Fe content: (a) 0, (b) 0.46 wt%, (c) 0.93 wt%, (d) 1.8 wt%, (e) 3.9 wt%.

Figure 4(C) shows the XRD traces of the used catalysts. XRD of used Pd–Pt/SZ showed peaks at 24.4°, 28.2°, and 31.4°, and smaller peaks between 39° and 46° and around 55° in addition to the peaks of the tetragonal phase at 30°, 35°, 50°, and 60°. The increase in the intensity of the 28° peak of the monoclinic phase after the durability test was also observed in Fe-doped samples, but the intensity of the peak decreased as Fe concentration increased.

The fractions of the monoclinic phase in the catalysts after the 500 °C durability tests were calculated based on the integrated intensity of the (101) reflection ($2\theta = 30.2°$) of the tetragonal phase and the intensities of the ($\bar{1}11$) ($2\theta = 28.2°$) and (111) ($2\theta = 31.4°$) reflections of the monoclinic phase, according to the equation of Toraya *et al.* [25]. The fractions of the monoclinic phase in the used Pd–Pt/SZ, Pd–Pt/0.46% Fe-SZ, Pd–Pt/0.93% Fe-SZ, and Pd–Pt/1.8% Fe-SZ were 42, 29, 18, and 9%, respectively. Successful band resolution could not be achieved for the used Pd–Pt/3.9% Fe-SZ because of the very small intensities of the monoclinic bands, but the fraction of the monoclinic phase in the sample was estimated to be below 5% from the integrated intensities of the 28.2° and 30.2° peaks. These XRD results indicate that a significant part of the tetragonal phase turns into the monoclinic phase during the test, and the addition of Fe stabilizes the tetragonal phase.

Figure 5 shows the Raman spectra of the fresh and used catalysts and reference materials. Sulfated zirconia showed bands at 269, 316, 459, 644 cm^{-1} which are assigned to tetragonal zirconia [21]. The band at 1032 cm^{-1} and shoulders at 1001 and 1250 cm^{-1} are assigned to the sulfate group. Smaller peaks at 179, 191, and 381 cm^{-1} indicate the presence of a trace amount of the monoclinic phase. Monoclinic zirconia showed bands at 179, 191, 223, 307, 333, 347, 382, 475, 501, 537, 558, 615, and 636 cm^{-1}. This is in agreement with previously reported results [26,27]. Iron oxide (α-Fe_2O_3) showed sharp bands at 224, 290, and 407 cm^{-1}, and smaller bands at 494 and 606 cm^{-1}, as well as a broad band at 1310 cm^{-1}. A 488.0 nm excited Raman spectrum of α-Fe_2O_3 (not shown) showed all these bands, but the intensity of the 1310 cm^{-1} band was much less. Therefore, the broad band may be related to defects and gains its intensity by the resonance effect. Palladium oxide showed a sharp Raman band at 645 cm^{-1}.

Fresh Pd–Pt/SZ showed Raman bands of the tetragonal zirconia (269, 316, 645 cm^{-1}, etc.). Small peaks at 382 cm^{-1}, etc., are assigned to the monoclinic zirconia. With an increase in the Fe content, the monoclinic band at 382 cm^{-1} decreased in intensity. In the Raman spectra of Pd–Pt/1.8% Fe-SZ and Pd–Pt/3.9% Fe-SZ, sharp bands were observed at 226, 292, and 409 cm^{-1}, which are assigned to α-Fe_2O_3. The presence of PdO was not determined partly because the most intense band of PdO (645 cm^{-1}) coincides with the strong peak of the tetragonal zirconia.

In the Raman spectra of the used catalysts, a large decrease in the intensity of the sulfate band at *ca.* 1030 cm^{-1} was observed for all samples. This is in agreement with the results of the chemical analysis. An

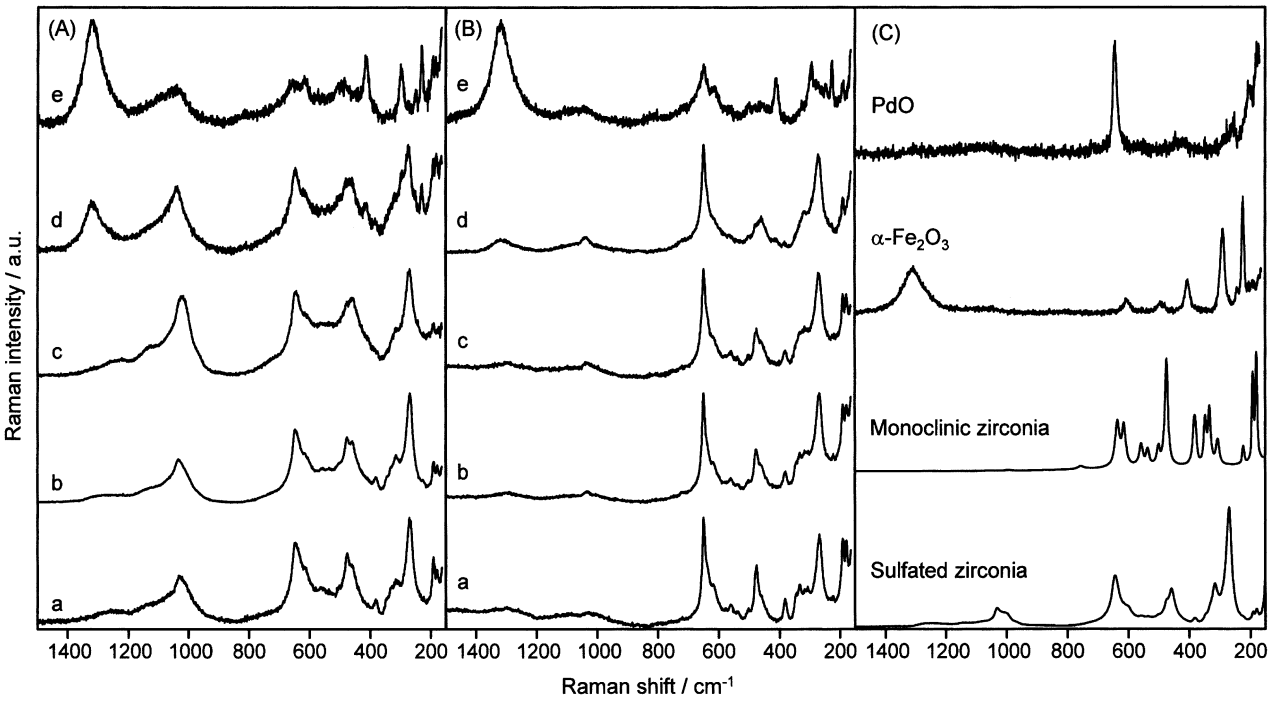

Figure 5. Raman spectra of (A) fresh catalysts, (B) used catalysts, and (C) reference materials: (a) Pd–Pt/SZ, (b) Pd–Pt/0.46% Fe-SZ, (c) Pd–Pt/0.93% Fe-SZ, (d) Pd–Pt/1.8% Fe-SZ, (e) Pd–Pt/3.9% Fe-SZ.

Table 3
Fraction of dispersed Pd determined by NaCl elution method

	Fresh catalyst (%)	Used catalyst [a] (%)
Pd–Pt/SZ	56	8.2
Pd–Pt/0.46% Fe-SZ	63	8.3
Pd–Pt/0.93% Fe-SZ	39	6.0
Pd–Pt/1.8% Fe-SZ	36	8.2
Pd–Pt/3.9% Fe-SZ	36	7.8

[a] After durability test at 500 °C.

increase in the intensity of the monoclinic band after the durability test and the suppression of the growth of the monoclinic phase by Fe were also observed in the Raman spectra. The bands of α-Fe_2O_3 were clearly observed in the Raman spectrum of Pd–Pt/3.9% Fe-SZ, but they were not clear in the spectrum of Pd–Pt/1.8% Fe-SZ.

When the shape and the intensity of the 645 cm^{-1} band are compared before and after the reaction test, the growth of an additional component with a sharp profile centered around 645 cm^{-1} is noticed for Pd–Pt/SZ, Pd–Pt/0.46% Fe-SZ, Pd–Pt/0.93% Fe-SZ, and Pd–Pt/1.8% Fe-SZ. This indicates the presence of agglomerated PdO in these samples. The quantitative determination of the fraction of the agglomerated PdO is difficult by Raman analysis, but the peak intensities suggest that the extent of PdO agglomeration is not much different among these samples.

Table 3 shows the fraction of Pd eluted by NaCl solution. Ogura *et al.* have shown that this method is effective for the determination of isolated Pd cations in Pd ion exchanged zeolites. They also reported that no elution of Pd has been observed for Pd/SiO_2 in which Pd was supported as agglomerated PdO. However, the applicability of this method to other supports and the effect of other metals such as Pt are not clear. Besides, whether intermediate species such as small PdO clusters are eluted or not is not clear. Therefore, "dispersed Pd" will be used in this report in place of "isolated Pd cation". The results show that 56% of the loaded Pd was dispersed Pd in fresh Pd–Pt/SZ. Since the fraction is almost one in highly dispersed Pd/zeolite, it may indicate that not all of the Pd is well dispersed, or interaction with Pt such as alloy formation may affect the state of Pd. After the durability tests, the fraction became less than 10%, which is in agreement with the Raman results and indicates that a significant part of the loaded Pd agglomerates to form PdO. The fraction of dispersed Pd on fresh Pd–Pt/Fe-doped SZ was 36–63%, which was not much different from the value of the fresh Pd–Pt/SZ. The decrease in the fraction of dispersed Pd after the durability test was similar to that of Pd–Pt/SZ. This shows that the addition of Fe does not significantly improve Pd dispersion.

4. Discussion

There seems to be a consensus that acid sites and dispersed Pd play key roles in the selective reduction of NO_x by methane on Pd-based catalysts [15,28–30]. Therefore, the following are considered to be the causes of deactivation: (i) agglomeration of dispersed Pd to form PdO, and (ii) deterioration of acid sites.

The agglomeration of dispersed Pd is clearly indicated by the decrease in the amount of dispersed Pd determined by the NaCl elution method and the Raman spectra of the fresh and used Pd–Pt/SZ. Since the acid sites of sulfated zirconia are formed by surface sulfate, the deterioration of acid sites means the loss of or structural changes in the sulfate. The loss of sulfate during the reaction is shown by the decrease in the amount of S after the tests. The stable phase of ZrO_2 is monoclinic below 1170 °C, and the tetragonal phase is stabilized by surface sulfate on SZ. Accordingly, the desorption of surface sulfate is considered to be the reason for the growth of the monoclinic phase after the test. While Pd-loaded SZ shows activity for NO_x reduction by methane [15], Pd-loaded ZrO_2 does not show significant activity for the reaction [31]. These facts suggest that the change of SZ to ZrO_2 is also a cause of the deactivation of Pd–Pt/SZ.

There is no direct evidence that the addition of Fe suppresses these deactivation mechanisms. The results of both the Raman spectra and the NaCl elution did not show any clear difference between Pd–Pt/SZ and Pd–Pt/Fe-SZ. The comparison of the S content after the 340 h durability tests shows that the added Fe contributes to the stabilization of surface sulfate. However, the S content of Pd–Pt/0.93% Fe-SZ after the 2400 h test and that of Pd–Pt/SZ after the 340 h test were similar, while the former catalyst showed much higher NO_x conversion than the latter. Therefore, the stabilization of surface sulfate by itself does not explain the effect of Fe against deactivation.

A clear difference between Pd–Pt/SZ and Pd–Pt/Fe-SZ was observed in the growth of the monoclinic phase after the tests. It is well known that divalent or trivalent cations such as Mg^{2+}, Ca^{2+}, Sc^{3+}, Y^{3+}, etc., stabilize cubic or tetragonal zirconia [32], and similar stabilization is also observed on Fe^{3+} [33]. Stefanic *et al.* reported that ZrO_2–Fe_2O_3 forms a solid solution, and the solubility limit of Fe_2O_3 in ZrO_2 is 4–6 mol% [34]. The state of Fe in Fe-doped SZ is still a matter of debate. Yamamoto *et al.* [22] measured Fe K-edge EXAFS and concluded that Fe formed an interstitial-type solid solution with ZrO_2 in Fe (1.1 wt%)-doped SZ. On the other hand, Scheithauer *et al.* [21] reported that Fe is present as supported Fe_2O_3 particles with a diameter of 1–2 nm in Fe (2 wt%)-doped SZ. It must be noted that Stefanic *et al.* prepared Fe_2O_3–ZrO_2 by co-precipitation, while Fe was loaded on zirconium hydroxide in this work and the works by Yamamoto *et al.* and Scheithauer

et al. The Raman result in this work is not necessarily inconsistent with these previous reports, when the differences in preparation are taken into account.

Another clear effect of Fe is the suppression of methane conversion. NO_x conversion on Pd–Pt/SZ goes through a maximum at 450 °C and decreases at higher temperatures because of methane consumption by simple oxidation [24]. On the other hand, in the case of Pd–Pt/0.93% Fe-SZ, NO_x conversion at 500 °C was much higher than that at 450 °C. These results suggest that the suppression of methane oxidation is related to the improvement in durability caused by the addition of Fe.

The above discussion leads to the following conclusions. Under actual exhaust conditions, Pd–Pt/SZ gradually deactivates. The deactivation is caused by the agglomeration of dispersed Pd to form PdO, the loss of surface sulfate, and the concomitant transformation of sulfated zirconia to monoclinic zirconia. The activity of Pd–Pt/Fe-doped SZ is more stable. The addition of Fe does not significantly suppress the agglomeration of Pd nor the loss of sulfate, but it does stabilize the tetragonal phase of zirconia. It also suppresses methane oxidation. Accordingly, the addition of Fe improves the selectivity for NO_x reduction, especially at higher temperatures.

It is still unclear whether the added Fe only suppresses the methane oxidation on agglomerated PdO, or whether it has any direct interaction with the dispersed Pd to improve the selectivity for NO_x reduction.

Lastly, the mechanism for the initial activation of Pd–Pt/Fe-doped SZ should be mentioned. As shown by XRD, the crystallinity of Fe-SZ is considerably lower than that of SZ, but it increased after the durability test. Hino and Arata investigated the effect of calcination temperature on the *n*-butane isomerization activity of SZ and Fe-SZ, and reported that the activity increases with the calcination temperature up to 650 °C for SZ and 700 °C for Fe-SZ [19,35]. The Fe-SZ in this work was calcined at a much lower temperature (550 °C), which suggests that the initial activiation of Pd–Pt/Fe-doped SZ is caused by the increase in the acidity accompanied by the increase in the crystallinity of Fe-SZ.

5. Conclusion

The effects of adding Fe on Pd–Pt/SZ for the selective NO_x reduction by methane were investigated. The addition of iron improved NO_x conversion at higher temperatures. 0.25% Pd–0.1% Pt/0.93% Fe-SZ maintained a NO_x conversion higher than 70% for over 2400 h at 500 °C. The effects of Fe were: (i) the suppression of methane conversion, which leads to increased NO_x conversion at higher temperatures, and (ii) the stabilization of the tetragonal phase over transformation to the monoclinic phase, which leads to improved durability.

Acknowledgment

The author wishes to thank Dr. Takenori Hirano of Kyushu Catalyst Research Inc. for many helpful discussions.

References

[1] Y. Li and J.N. Armor, Appl. Catal. B 1 (1992) L31.
[2] Y. Li and J.N. Armor, Appl. Catal. B 2 (1993) 239.
[3] E. Kikuchi and K. Yogo, Catal. Today 22 (1994) 73.
[4] Y. Li and J.N. Armor, J. Catal. 145 (1994) 1.
[5] Y. Nishizaka and M. Misono, Chem. Lett. (1993) 1295.
[6] Y. Nishizaka and M. Misono, Chem. Lett. (1994) 2237.
[7] H. Uchida, K. Yamaseki and I. Takahashi, Catal. Today 29 (1996) 99.
[8] J.N. Armor, Catal. Today 26 (1995) 147.
[9] S. Satokawa, K. Yamaseki and H. Uchida, Proc. Meeting of the Japan Association of Zeolite 15 (1999) 104.
[10] M. Suzuki, J. Amano and M. Niwa, Microporous Mesoporous Mater. 21 (1998) 541.
[11] M. Ogura, Y. Sugiura, M. Hayashi and E. Kikuchi, Catal. Lett. 42 (1996) 185.
[12] M. Ogura, S. Kage, M. Hayashi, H. Matsukata and E. Kikuchi, Appl. Catal. B 27 (2000) L213.
[13] H. Hamada, Y. Kintaichi, M. Tabata, M. Sasaki and T. Ito, Shokubai (Catalyst) 33 (1991) 59.
[14] H. Hamada, Shokubai (Catalyst) 33 (1991) 320.
[15] C.J. Loughran and D.E. Resasco, Appl. Catal. B 7 (1995) 113.
[16] Y.-H. Chin, W.E. Alvarez and D.E. Resasco, Catal. Today 62 (2000) 159.
[17] J.K. Lampert, M.S. Kazi and R.J. Farrauto, Appl. Catal. B 14 (1997) 211.
[18] H. Ohtsuka, T. Tabata and T. Hirano, Appl. Catal. B 28 (2000) L73.
[19] M. Hino and K. Arata, Hyomen (Surface) 34 (1996) 51.
[20] K. Arata, Appl. Catal. A 146 (1996) 3.
[21] M. Scheithauer, E. Bosch, U.A. Schubert, H. Knoezinger, T.-K. Cheung, F.C. Jentoft, B.C. Gates and B. Tesche, J. Catal. 177 (1998) 137.
[22] T. Yamamoto, T. Tanaka, S. Takenaka, S. Yoshida, T. Onari, Y. Takahashi, T. Kosaka, S. Hasegawa and M. Kudo, J. Phys. Chem. B 103 (1999) 2385.
[23] M. Ogura, M. Hayashi and E. Kikuchi, Proc. 12th Int. Zeolite Conference, 5–10 July 1998, Baltimore, MD, p. 2833.
[24] H. Ohtsuka and T. Tabata, Appl. Catal. B 29 (2001) 177.
[25] H. Toraya, M. Yoshimura and S. Somiya, J. Am. Ceram. Soc. 67 (1984) C-119.
[26] E. Anastassakis, B. Papanicolaou and I.M. Asher, J. Phys. Chem. Solids 36 (1975) 667.
[27] C. Carlone, Phys. Rev. B 45 (1992) 2079.
[28] G. Koyano, S. Yokoyama and M. Misono, Appl. Catal. A 188 (1999) 301.
[29] M. Ogura, M. Hayashi, S. Kage, M. Matsukata and E. Kikuchi, Appl. Catal. B 23 (1999) 247.
[30] B.J. Adelman and W.M.H. Sachtler, Appl. Catal. B 14 (1997) 1.
[31] M. Inaba, Y. Kintaichi, M. Haneda and H. Hamada, Nihon Kagaku Kaishi (2000) 467.
[32] E.C. Subbarao, in: *Advances in Ceramics*, Vol. 3, eds. H. Heuer and L.W. Hobbs (American Ceramics Society, Columbus, OH, 1981) p. 1.
[33] M. Lajavardi, D.J. Kenney and S.H. Lin, J. Chinese Chem. Soc. 47 (2000) 1065.
[34] G. Stefanic, S. Music, S. Popovic and K. Nomura, J. Mol. Struct. 480–481 (1999) 627.
[35] M. Hino and K. Arata, Hyomen (Surface) 28 (1990) 481.